



1 **Climatic subdivision of Heinrich Stadial 1 based on**
2 **centennial-scale paleoenvironmental changes observed**
3 **in the western Mediterranean area**

4 **Jon Camuera^{1, 2}, Gonzalo Jiménez-Moreno², María J. Ramos-Román¹, Antonio**
5 **García-Alix^{2, 3}, Francisco Jiménez-Espejo³, Jaime L. Toney⁴, R. Scott Anderson⁵,**
6 **Cole Webster⁵**

7 ¹ *Department of Geosciences and Geography, Faculty of Science, University of Helsinki, Finland*

8 ² *Departamento de Estratigrafía y Paleontología, Universidad de Granada, Spain*

9 ³ *Instituto Andaluz de Ciencias de la Tierra (IACT), Consejo Superior de Investigaciones*
10 *Científicas-Universidad de Granada (CSIC-UGR), Granada, Spain*

11 ⁴ *School of Geographical and Earth Sciences, University of Glasgow, UK*

12 ⁵ *School of Earth and Sustainability, Northern Arizona University, USA*

13 Correspondence to: jon.camuera@helsinki.fi

14 Keywords: Climate, Heinrich Stadial 1, deglaciation, western Mediterranean, solar
15 activity

16 **ABSTRACT**

17 Heinrich Stadial 1 (HS1) is one of the most extreme climate periods of the last
18 glacial cycle, generating extremely low sea surface temperatures (SST) and significant
19 changes in terrestrial landscape (e.g., vegetation). Previous studies show that overall
20 cold/dry conditions occurred during HS1, but the lack of high-resolution records
21 precludes whether climate was stable or instead characterized by instability. A high-
22 resolution paleoclimatic record from Padul (southern Iberian Peninsula), supported by a
23 robust chronology, shows that climate during HS1 was non-stationary and centennial-



scale variability in moisture is superimposed on this overall cold climatic period. In this study we improve the resolution and suggest a novel subdivision of HS1 in 7 sub-phases, including: i) 3 sub-phases (a.1–a.3) during an arid early phase (HS1a; ~18.4–17.2 kyr BP), ii) a humid middle phase (HS1b; ~17.2–16.7 kyr BP), and iii) 3 sub-phases (c.1–c.3) during an arid late phase (HS1c; ~16.7–15.6 kyr BP). This climatic subdivision is regionally supported by SST oscillations from the Mediterranean Sea, suggesting a strong land-ocean relationship. A cyclostratigraphic analysis of our pollen data indicates that HS1 climate variability, and thus this subdivision, is characterized by ~2000 and ~800-yr periodicities, suggesting solar forcing controlling climate in this area.

INTRODUCTION

Understanding the background of natural climatic variability underlying abrupt anthropogenic climate change is a main goal in paleoclimate research. In this respect, deciphering rapid (e.g., millennial-scale) climate change and environmental impacts due to Dansgaard/Oeschger (D/O) and Heinrich-like climatic oscillations during the last glacial period and deglaciation have been the aim of ice, marine and terrestrial paleoclimate investigations (Cacho et al., 2006; Höbig et al., 2012; Panagiotopoulos et al., 2014).

Several paleoclimatic records evidenced the effect of especially cold and arid conditions recorded during Heinrich Stadials (HSs) in marine and terrestrial environments (Fletcher and Sánchez Goñi, 2008; Moreno et al., 2010; Martrat et al., 2014; Hodell et al., 2017). High-resolution paleoclimatic records also show that climate during HS1 was characterized by short-scale internal variability (Dupont et al., 2010; Stager et al., 2011; Escobar et al., 2012; Zhang et al., 2014; Stríkis et al., 2015). However, few studies focus on short-scale internal climate variability of HSs in southern Europe and the Mediterranean region, and in particular within HS1 (Fletcher and Sánchez Goñi, 2008).



49 In this regard, a division of HS1 into two and three phases has previously been observed
 50 in very few marine records (Supplementary Information and Table S1). Nevertheless, the
 51 studies showing a three-phase division of HS1 disagree in the paleoenvironmental
 52 characterization of each phase (Table S1) and a complete knowledge of the variability
 53 within HS1 has yet to be achieved (Hodell et al., 2017).

54 Here, we present pollen and sedimentation data between 20 and 11 kyr BP from
 55 the new Padul-15-05 terrestrial sedimentary record (southern Iberian Peninsula; Fig. 1),
 56 registering regional and local paleoenvironmental responses to climate changes during
 57 HS1 and deglaciation, i.e., Bølling-Allerød (BA) and Younger Dryas (YD). The high-
 58 resolution data (~61-yr) from 18.4 to 15.6 kyr BP revealed centennial-scale variability
 59 during HS1, which is replicated in other Mediterranean paleoclimatic records and enables
 60 us to suggest, for the first time, an accurate internal climatic subdivision of HS1.

61 MATERIALS AND METHODS

62 In this study we used 10 AMS radiocarbon dates to obtain an accurate
 63 chronological control between 20 and 11 kyr BP from the Padul-15-05 record (Fig. 2a
 64 and Table S2; Supplementary Information for more precise methodology).

65 The Mediterranean forest, xerophytes, Pollen Climate Index (PCI) and
 66 Precipitation Index (I_p) were used as pollen paleoclimatic proxies (Fig. 2c-f and Fig. 3a).
 67 The PCI is useful for temperature and precipitation related climate changes, whereas I_p is
 68 a proxy for precipitation reconstruction in this region. In addition, normalized silicon
 69 (Si_{norm}) data from XRF analysis (Fig. 2b) was used as indicator of the siliciclastic input
 70 from the Sierra Nevada into the wetland (Camuera et al., 2018) (Methods, Supplementary
 71 Information).

72 For the purpose of identifying cyclicities related to regional climate oscillations,
 73 a cyclostratigraphic spectral analysis using the REDFIT procedure under rectangular



74 window function from (Schulz and Mudelsee, 2002) was performed on xerophyte and *Ip*
75 data, which have been proven to be good proxies for regional moisture availability in this
76 area (Pini et al., 2009; Fletcher et al., 2010). A spectral analysis was also run on raw GRIP
77 ¹⁰Be flux data between 18.6 and 11 kyr BP (Adolphi et al., 2014) in order to observe
78 cyclicities related to solar activity (Fig. 4; Methods, Supplementary Information).

79 RESULTS AND DISCUSSION

80 Heinrich Stadial 1 (HS1)

81 The terrestrial paleoclimate record from Padul shows overall cold and arid
82 conditions during HS1, deduced by the decrease in mesic forest and abundance of
83 xerophytes between 18.4 and 15.6 kyr BP (Fig. 2c, d). Centennial-scale variability is also
84 observed during HS1 that can be divided into 3 main climatic phases (i.e., HS1a from
85 18.4 to 17.2 kyr BP, HS1b from 17.2 to 16.7 kyr BP, and HS1c from 16.7 to 15.6 kyr BP)
86 and a further subdivision in 7 smaller-scale phases within them (i.e., HS1a.1, HS1a.2,
87 HS1a.3, HS1b, HS1c.1, HS1c.2 and HS1c.3) (Fig. 2e, f and Fig. 3a).

88 The first of the three main climatic phases in Padul, HS1a (early HS1; 18.4–17.2
89 kyr BP), is characterized by low temperatures with significant variability in precipitation
90 but under generally arid conditions, deduced by high xerophytes and low PCI and *Ip*
91 values (Fig. 2c, e, f). Especially cold/arid conditions during this early phase are confirmed
92 by high Si_{norm} values, which show that high siliciclastic input from the Sierra Nevada
93 range into the wetland are caused by enhanced erosion during decreased forest cover
94 (Camuera et al., 2019). The general cold/arid conditions shown in Padul during the early
95 HS1a were also documented in nearby marine records presenting the 3 main phases for
96 HS1, such as the pollen records from NW Iberia (Naughton et al., 2016), or the pollen
97 data, SST reconstructions and foraminifera/coccolithophore assemblages from Alboran
98 Sea (Fletcher and Sánchez Goñi, 2008; Martrat et al., 2014; Bazzicalupo et al., 2018).



99 HS1b (middle HS1; 17.2–16.7 kyr BP) is characterized in Padul by a moderate
 100 increase in temperature and precipitation, deduced by low xerophytes, and higher PCI
 101 and I_p values. This is further supported by low $S_{i\text{norm}}$, indicative of low erosion precluding
 102 siliciclastic input in the wetland (Fig. 2b, c, e, f). A similar slightly warmer climate during
 103 this phase was recorded in SST records from the Mediterranean (Cacho et al., 1999;
 104 2006), and in particular, from Alboran Sea (Martrat et al., 2014) (Fig. 3b and c, subjected
 105 to age uncertainties for onset/ending of HS1). This warmer/wetter conditions agree with
 106 increases in temperate forest recorded in the Iberian margin (Daniau et al., 2007), and in
 107 runoff in Lake Estanya (NE Spain) (Morellón et al., 2009).

108 HS1c (late HS1; 16.7–15.6 kyr BP) was climatically similar to HS1a,
 109 characterized by cold/dry conditions. This is deduced by the observed increase in
 110 xerophytes and $S_{i\text{norm}}$ and lowering in I_p between ~16.9 and 15.8 kyr BP, related with the
 111 decreasing moisture (Fig. 2b, c, e). The general cold/arid climate in Padul during this
 112 phase is concordant with low SST from Alboran Sea (Martrat et al., 2014) (Fig. 3a, b),
 113 and with increasing salinity and low lake level in Lake Estanya (Morellón et al., 2009).

114 Our high-resolution record also revealed shorter centennial-scale climatic
 115 variability during HS1a and HS1c with a further climatic subdivision of HS1 into 7 sub-
 116 phases (i.e., HS1a.1, HS1a.2, HS1a.3, HS1b, HS1c.1, HS1c.2 and HS1c.3):

117 HS1a.1 was characterized by a cold/arid phase between 18.4 and 17.8 kyr BP
 118 recorded by high xerophytes, and low PCI and I_p values. Climate changed towards more
 119 humidity in HS1a.2 sub-phase at 17.8–17.5 kyr BP, and returned to enhanced aridity
 120 during HS1a.3 between 17.5–17.2 kyr BP. This arid-humid-arid climatic pattern is further
 121 confirmed by oscillations in $S_{i\text{norm}}$ (Fig. 2b, c, e, f and Fig. 3a).

122 HS1c also presents a three-phase subdivision, namely HS1c.1, HS1c.2 and
 123 HS1c.3. HS1c.1 was characterized by a decrease in precipitation and temperature (low I_p



124 and lowest PCI values), registering the coldest conditions of HS1 at 16.7–16.4 kyr BP
 125 (Fig. 2f). Temperature and moisture conditions increased during HS1c.2 at 16.4–16 kyr
 126 BP, whereas similar temperatures but under more arid climate conditions are recorded
 127 during HS1c.3 at 16–15.6 kyr BP (Fig. 2c, e, f and Fig. 3a). This arid-humid-arid climatic
 128 pattern is similar to the earlier HS1a.

129 Environmental changes recorded in Padul represent centennial-scale climate
 130 oscillations during HS1, which can be correlated with other regional records. The
 131 centennial-scale arid-humid-arid trends recorded during HS1a and HS1c, and the increase
 132 in temperature/precipitation during HS1b, are also observed in the SST records from the
 133 Alboran Sea in western Mediterranean (Cacho et al., 1999; 2006; Martrat et al., 2014)
 134 and in the GISP2 ice core (Grootes et al., 1993) (Fig. 3a-d), suggesting a similar response
 135 in continental, marine and ice sheet environments to climatic forcing (see section below).
 136 The presented age offsets between records could be related with variations in reservoir
 137 ages of the Atlantic and Mediterranean promoted by thermohaline circulation collapse in
 138 both areas during HS1 (Sierro et al., 2005). In addition, the significant decrease in the
 139 atmospheric ^{14}C between 17.5 and 14.5 kyr also difficult age models during this period
 140 (Broecker and Barker, 2007), whereas dating on different foraminifera species can also
 141 produce large differences on radiocarbon ages, especially during HS1 (up to 1000 years)
 142 (Ausín et al., 2019). The asynchronicity and the early record of HS1 in Padul (18.4–15.6
 143 kyr BP) with respect to the equivalent GS-2.1a cold event from Greenland ice-core
 144 records (17.5–14.7 kyr BP) is evident. This could be due to different environmental
 145 responses consequence of the different latitude and geographical features between high-
 146 latitude Greenland and mid-latitude Mediterranean and Iberian records. An early record
 147 of HS1 in the study area is supported by the well-dated paleoenvironmental records from
 148 our region. For instance, the growth interruption of the CAN speleothem (N Spain)



149 occurred between 18.2 and 15.4 kyr BP (Moreno et al., 2010) supporting an early HS1
150 (or Mystery Interval in their study), the increasing moisture conditions in Lake Prespa
151 (Macedonia, Albania, Greece) at 15.7 kyr BP indicating an early end of HS1 (Cvetkoska
152 et al., 2015), and the pollen record from MD99-2331 (NW Iberian margin), which
153 evidence HS1 between 18.8 and 15.8 kyr BP (Sánchez Goñi et al., 2018).

154 Despite the offsets of SST reconstructions from Mediterranean Sea,
155 environmental oscillations in both areas should have been synchronous. Therefore,
156 warming peaks recorded in Padul and in SST records during HS1 were coetaneous, result
157 of the strong land-ocean interaction (Sánchez Goñi et al., 2018).

158 **Bølling-Allerød (BA) and Younger Dryas (YD)**

159 The BA recorded in Padul between 15.6 and 12.9 kyr BP is characterized by
160 significant increase in the Mediterranean forest, and thus *Ip* and PCI values, indicating
161 warmer/wetter climate than during HS1. In addition, Padul is one of the few continental
162 records to detect the 5 centennial-scale sub-phases during the BA, similar to the GI-1e to
163 GI-1a from Greenland ice cores (Johnsen et al., 1992; Grootes et al., 1993) (Fig. 2e, f and
164 Fig. 3d).

165 Cold/arid climate during the YD stadial also affected the paleoenvironments in
166 this area between 12.9–11.6 kyr BP. The YD is characterized by relatively arid conditions
167 show by the mean xerophyte percentage of ~22%, whereas temperature seems to increase
168 throughout the YD period, reflected by the increasing trend in the Mediterranean forest
169 (Fig. 2c, d).

170 **Climate variability and solar forcing in the Iberian Peninsula**

171 Centennial- and millennial-scale climate variability have been recorded during
172 HS1, BA and YD period in Padul. The spectral analysis on xerophytes and *Ip* presented
173 ~2000, 800, 500 and 200-yr cycles (Fig. 4a-c). These climatic variabilities could be



related to solar forcing, as similar cyclicities have been obtained analyzing solar activity with ^{14}C production rates (Damon and Jirikowic, 1992; Turney et al., 2005). Several studies have determined a relation between paleoenvironmental data oscillations linked to climate changes through variations in solar activity (Bond et al., 2001; Lüning and Vahrenholt, 2016). In particular, climate variability during the Last Glacial and Holocene periods was strongly controlled by solar activity, specifically during cold glacial phases, in which solar variability caused larger climate changes (van Geel et al., 1999). In addition, more recent temperature estimations showed that they also seem to be forced by solar variability (Soon et al., 2015).

The obtained ~2000-yr climatic cyclicity forced millennial-scale paleoenvironmental variability in Padul and permitted the three-phase division of HS1 (Fig. 5a, b). This cyclicity could be linked to D/O-like variability, which presents a 1–2 kyr periodicity during the last glaciation (Bond et al., 1999), such as the ~1.8-kyr cycle identified on the hematite-stained grain record from North Atlantic cores (Bond et al., 1999). Paleoclimatic records from the Equator and Southern Hemisphere also determined periodic surface temperature variations of around 2000 yrs in relation with solar irradiance (Bütikofer, 2007).

The ~800-yr cycle identified in Padul forced the centennial-scale climatic subdivision of HS1 in 7 sub-phases (Fig. 5a, c). A similar ~800 yr cyclicity characterizes the ^{10}Be flux data indicative of changes in solar activity (Adolphi et al., 2014) (Fig. 4d and Fig. 5d, e). Other global paleoclimatic studies also show similar frequencies caused by solar variability. For example, an ~800-yr cycle was observed in Irish oak tree chronologies (Turney et al., 2005) and in Mg/Ca SST from the Pacific Ocean (Marchitto et al., 2010), both records closely related to solar irradiance. A 890-yr cycle was also found in the $\delta^{18}\text{O}$ Holocene time series from Greenland and interpreted as linked to solar



199 radiation (Schulz and Paul, 2002). Consequently, the ~800-yr cycle detected in Padul and
200 in other worldwide records suggests a linkage between centennial-scale
201 paleoenvironmental changes and solar activity.

202 The data from Padul display a good correlation between environmental changes
203 in the southern Iberian Peninsula and Mediterranean SSTs during HS1 (Fig. 3a-c),
204 suggesting a close land-ocean relationship in response to solar variability. The
205 Mediterranean SST could have been affected by solar activity, similar to the North
206 Atlantic cooling episodes linked to reduced solar irradiance (Bond et al., 2001). In
207 addition, observed variations in the Padul data suggest a southward shift of the North
208 Atlantic polar front during HS1 (Repschläger et al., 2015), which could have produced a
209 penetration of colder Atlantic surface waters into the Mediterranean (Cacho et al., 1999;
210 Sierro et al., 2005). These conditions, along with the southward displacement of the North
211 Atlantic atmospheric polar front, could have produced a low land-ocean temperature
212 contrast and weak moisture advection between both environments, and therefore,
213 increasing aridity in the western Mediterranean during cold sub-phases HS1a.1, HS1a.3,
214 HS1c.1 and HS1c.3. Similar conditions linked to weak moisture advection were
215 interpreted in the eastern Mediterranean during HS1 and HS2 (Kwiecien et al., 2009) and
216 in the Corchia Cave during HS11 (Drysedale et al., 2009). In contrast, during warmer sub-
217 phases in Padul (i.e., HS1a.2, HS1b and HS1c.2) and in Mediterranean SSTs, enhanced
218 marine evaporation and moisture advection toward the continent could have provoked
219 wetter climate conditions in southern Iberian Peninsula.

220 CONCLUSIONS

221 The high-resolution analysis of the Padul-15-05 continental record for the 20–11
222 kyr BP interval shows that:



- 223 1) Centennial-scale climate oscillations affected southern Iberian Peninsula
 224 during HS1, with three main phases HS1a (18.4–17.2 kyr BP), HS1b (17.2–
 225 16.7 kyr BP) and HS1c (16.7–15.6 kyr BP) characterized by general
 226 arid(cold), humid(cool) and arid(cold) climate, respectively.
- 227 2) We suggest for the first time a further subdivision within these 3 main climatic
 228 phases of HS1 in 7 sub-phases: 3 sub-phases (a.1–a.3) during HS1a, HS1b,
 229 and 3 sub-phases (c.1–c.3) during HS1c. The climatic variability is also
 230 identified in Mediterranean SST records, confirming this climatic pattern at
 231 regional-scale.
- 232 3) The main periodicities obtained for climatic oscillations of ~2000 and ~800
 233 yrs within HS1, BA and YD seem to be related to solar forcing. Variations in
 234 solar activity could have influenced latitudinal shifts of the North Atlantic and
 235 atmospheric polar fronts, affecting the land-ocean temperature contrast,
 236 marine evaporation and moisture advection toward the continent.

237 **ACKNOWLEDGMENTS**

238 This research is supported by the projects CGL2013-47038-R and CGL-2017-
 239 85415-R, PhD funding BES-2014-069117 (Jon Camuera) and Ramón y Cajal fellowship
 240 RYC-2015-18966 (Antonio García-Alix) provided by the Ministerio de Economía y
 241 Competitividad of the Spanish Government. Additional funding was provided by the
 242 research group RNM0190 and the project P11-RNM-7332 with a postdoctoral fellowship
 243 (María J. Ramos-Román) from the Junta de Andalucía.

244 **DATA AVAILABILITY**

245 The paleoclimatic pollen data from Padul-15-05 can be found in the PANGAEA
 246 data repository (<https://doi.pangaea.de/10.1594/PANGAEA.904053>, dataset *in review*).



247 AUTHOR CONTRIBUTIONS

248 J.C. performed the pollen, XRF and spectral analyses, interpreted the data and
 249 wrote the manuscript. G.J.-M. discussed data and interpretations and wrote the
 250 manuscript. M.J.R.-R. performed the XRF analysis, discussed data and interpretations
 251 and contributed to the writing of the manuscript. A.G.-A., J.L.T., R.S.A., F.J.E. and C.W.
 252 discussed data and interpretations and contributed to the writing of the manuscript.

253 COMPETING INTEREST

254 The authors declare no financial and non-financial competing interests.

255

256 REFERENCES

257

258 Adolphi, F., Muscheler, R., Svensson, A., Aldahan, A., Possnert, G., Beer, J., Sjolte,
 259 J., Björck, S., Matthes, K., and Thiéblemont, R.: Persistent link between solar activity and
 260 Greenland climate during the Last Glacial Maximum, *Nature Geoscience*, 7, 662,
 261 <https://doi.org/10.1038/NGEO2225>, 2014.

262 Ausín, B., Haghpor, N., Wacker, L., Voelker, A. H., Hodell, D., Magill, C., Looser,
 263 N., Bernasconi, S. M., and Eglinton, T. I.: Radiocarbon age offsets between two surface
 264 dwelling planktonic foraminifera species during abrupt climate events in the SW Iberian
 265 margin, *Paleoceanography* and *Paleoclimatology*,
 266 <https://doi.org/10.1029/2018PA003490>, 2019.

267 Bazzicalupo, P., Maiorano, P., Girone, A., Marino, M., Combourieu-Nebout, N., and
 268 Incarbona, A.: High-frequency climate fluctuations over the last deglaciation in the
 269 Alboran Sea, Western Mediterranean: Evidence from calcareous plankton assemblages,
 270 *Palaeogeography, Palaeoclimatology, Palaeoecology*, 506, 226-241,
 271 <https://doi.org/10.1016/j.palaeo.2018.06.042>, 2018.

272 Bond, G., Kromer, B., Beer, J., Muscheler, R., Evans, M. N., Showers, W.,
 273 Hoffmann, S., Lotti-Bond, R., Hajdas, I., and Bonani, G.: Persistent solar influence on



- 274 North Atlantic climate during the Holocene, *Science*, 294, 2130-2136,
 275 <https://doi.org/10.1126/science.1065680>, 2001.
- 276 Bond, G. C., Showers, W., Elliot, M., Evans, M., Lotti, R., Hajdas, I., Bonani, G.,
 277 and Johnson, S.: The North Atlantic's 1-2 kyr climate rhythm: relation to Heinrich events,
 278 Dansgaard/Oeschger cycles and the Little Ice Age, *Mechanisms of global climate change*
 279 at millennial time scales, 112, 35-58, <https://doi.org/10.1029/GM112p0035>, 1999.
- 280 Broecker, W., and Barker, S.: A 190‰ drop in atmosphere's $\Delta^{14}\text{C}$ during the
 281 “Mystery Interval”(17.5 to 14.5 kyr), *Earth and Planetary Science Letters*, 256, 90-99,
 282 <https://doi.org/10.1016/j.epsl.2007.01.015>, 2007.
- 283 Büttikofer, J.: Millennial scale climate variability during the last 6000 years—tracking
 284 down the Bond cycles, University of Bern, 124 pp., 2007.
- 285 Cacho, I., Grimalt, J. O., Pelejero, C., Canals, M., Sierro, F. J., Flores, J. A., and
 286 Shackleton, N.: Dansgaard-Oeschger and Heinrich event imprints in Alboran Sea
 287 paleotemperatures, *Paleoceanography*, 14, 698-705,
 288 <https://doi.org/10.1029/1999PA900044>, 1999.
- 289 Cacho, I., Shackleton, N., Elderfield, H., Sierro, F. J., and Grimalt, J. O.: Glacial
 290 rapid variability in deep-water temperature and $\delta^{18}\text{O}$ from the Western Mediterranean
 291 Sea, *Quaternary Science Reviews*, 25, 3294-3311,
 292 <https://doi.org/10.1016/j.quascirev.2006.10.004>, 2006.
- 293 Camuera, J., Jiménez-Moreno, G., Ramos-Román, M. J., García-Alix, A., Toney, J.
 294 L., Anderson, R. S., Jiménez-Espejo, F., Kaufman, D., Bright, J., and Webster, C.:
 295 Orbital-scale environmental and climatic changes recorded in a new ~ 200,000-year-long
 296 multiproxy sedimentary record from Padul, southern Iberian Peninsula, *Quaternary*
 297 *Science Reviews*, 198, 91-114, <https://doi.org/10.1016/j.quascirev.2018.08.014>, 2018.
- 298 Camuera, J., Jiménez-Moreno, G., Ramos-Román, M. J., García-Alix, A., Toney, J.
 299 L., Anderson, R. S., Jiménez-Espejo, F., Bright, J., Webster, C., and Yanes, Y.:
 300 Vegetation and climate changes during the last two glacial-interglacial cycles in the
 301 western Mediterranean: A new long pollen record from Padul (southern Iberian
 302 Peninsula), *Quaternary Science Reviews*, 205, 86-105,
 303 <https://doi.org/10.1016/j.quascirev.2018.12.013>, 2019.



- 304 Cvetkoska, A., Levkov, Z., Reed, J. M., Wagner, B., Panagiotopoulos, K., Leng, M.
 305 J., and Lacey, J. H.: Quaternary climate change and Heinrich events in the southern
 306 Balkans: Lake Prespa diatom palaeolimnology from the last interglacial to present,
 307 Journal of Paleolimnology, 53, 215-231, <https://doi.org/10.1007/s10933-014-9821-3>,
 308 2015.
- 309 Damon, P. E., and Jirikowic, J. L.: The sun as a low-frequency harmonic oscillator,
 310 Radiocarbon, 34, 199-205, <https://doi.org/10.1017/S003382220001362X>, 1992.
- 311 Daniau, A.-L., Sánchez-Goñi, M., Beaufort, L., Laggoun-Défarge, F., Loutre, M.-F.,
 312 and Duprat, J.: Dansgaard-Oeschger climatic variability revealed by fire emissions in
 313 southwestern Iberia, Quaternary Science Reviews, 26, 1369-1383,
 314 <https://doi.org/10.1016/j.quascirev.2007.02.005>, 2007.
- 315 Drysdale, R., Hellstrom, J., Zanchetta, G., Fallick, A., Goñi, M. S., Couchoud, I.,
 316 McDonald, J., Maas, R., Lohmann, G., and Isola, I.: Evidence for obliquity forcing of
 317 glacial termination II, Science, 325, 1527-1531, <https://doi.org/10.1126/science.1170371>,
 318 2009.
- 319 Dupont, L. M., Schlütz, F., Ewah, C. T., Jennerjahn, T. C., Paul, A., and Behling, H.:
 320 Two-step vegetation response to enhanced precipitation in Northeast Brazil during
 321 Heinrich event 1, Global Change Biology, 16, 1647-1660, <https://doi.org/10.1111/j.1365-2486.2009.02023.x>, 2010.
- 323 Escobar, J., Hodell, D. A., Brenner, M., Curtis, J. H., Gilli, A., Mueller, A. D.,
 324 Anselmetti, F. S., Ariztegui, D., Grzesik, D. A., Pérez, L., Schwalb, A., and Guilderson,
 325 T. P.: A ~43-ka record of paleoenvironmental change in the Central American lowlands
 326 inferred from stable isotopes of lacustrine ostracods, Quaternary Science Reviews, 37,
 327 92-104, <https://doi.org/10.1016/j.quascirev.2012.01.020>, 2012.
- 328 Fletcher, W. J., and Sánchez Goñi, M. F.: Orbital- and sub-orbital-scale climate
 329 impacts on vegetation of the western Mediterranean basin over the last 48,000 yr,
 330 Quaternary Research, 70, 451-464, <https://doi.org/10.1016/j.yqres.2008.07.002>, 2008.
- 331 Fletcher, W. J., Sánchez Goñi, M. F., Peyron, O., and Dormoy, I.: Abrupt climate
 332 changes of the last deglaciation detected in a Western Mediterranean forest record,
 333 Climate of the Past, 6, 245-264, <https://doi.org/10.5194/cp-6-245-2010>, 2010.



334 Grootes, P. M., Stuiver, M., White, J., Johnsen, S., and Jouzel, J.: Comparison of
335 oxygen isotope records from the GISP2 and GRIP Greenland ice cores, *Nature*, 366, 552,
336 1993.

337 Högberg, N., Weber, M. E., Kehl, M., Weniger, G.-C., Julià, R., Melles, M., Fülöp, R.-
338 H., Vogel, H., and Reicherter, K.: Lake Banyoles (northeastern Spain): A Last Glacial to
339 Holocene multi-proxy study with regard to environmental variability and human
340 occupation, *Quaternary International*, 274, 205-218,
341 <https://doi.org/10.1016/j.quaint.2012.05.036>, 2012.

342 Hodell, D. A., Nicholl, J. A., Bontognali, T. R., Danino, S., Dorador, J., Dowdeswell,
343 J. A., Einsle, J., Kuhlmann, H., Martrat, B., and Mlenek-Vautravers, M. J.: Anatomy of
344 Heinrich layer 1 and its role in the last deglaciation, *Paleoceanography*, 32, 284-303,
345 <https://doi.org/10.1002/2016PA003028>, 2017.

346 Johnsen, S., Clausen, H. B., Dansgaard, W., Fuhrer, K., Gundestrup, N., Hammer,
347 C. U., Iversen, P., Jouzel, J., and Stauffer, B.: Irregular glacial interstadials recorded in a
348 new Greenland ice core, *Nature*, 359, 311, <https://doi.org/10.1038/359311a0>, 1992.

349 Kwiecien, O., Arz, H. W., Lamy, F., Plessen, B., Bahr, A., and Haug, G. H.: North
350 Atlantic control on precipitation pattern in the eastern Mediterranean/Black Sea region
351 during the last glacial, *Quaternary Research*, 71, 375-384,
352 <https://doi.org/10.1016/j.yqres.2008.12.004>, 2009.

353 Lüning, S., and Vahrenholt, F.: Chapter 16 - The Sun's Role in Climate, in: Evidence-
354 Based Climate Science (Second Edition), edited by: Easterbrook, D. J., Elsevier, 283-
355 305, 2016.

356 Marchitto, T. M., Muscheler, R., Ortiz, J. D., Carriquiry, J. D., and van Geen, A.:
357 Dynamical response of the tropical Pacific Ocean to solar forcing during the early
358 Holocene, *Science*, 330, 1378-1381, <https://doi.org/10.1126/science.1194887>, 2010.

359 Martrat, B., Jimenez-Amat, P., Zahn, R., and Grimalt, J. O.: Similarities and
360 dissimilarities between the last two deglaciations and interglaciations in the North
361 Atlantic region, *Quaternary Science Reviews*, 99, 122-134,
362 <https://doi.org/10.1016/j.quascirev.2014.06.016>, 2014.



- 363 Morellón, M., Valero-Garcés, B., Vegas-Vilarrúbia, T., González-Sampériz, P.,
 364 Romero, Ó., Delgado-Huertas, A., Mata, P., Moreno, A., Rico, M., and Corella, J. P.:
 365 Lateglacial and Holocene palaeohydrology in the western Mediterranean region: The
 366 Lake Estanya record (NE Spain), *Quaternary Science Reviews*, 28, 2582-2599,
 367 <https://doi.org/10.1016/j.quascirev.2009.05.014>, 2009.
- 368 Moreno, A., Stoll, H., Jiménez-Sánchez, M., Cacho, I., Valero-Garcés, B., Ito, E.,
 369 and Edwards, R. L.: A speleothem record of glacial (25–11.6kyr BP) rapid climatic
 370 changes from northern Iberian Peninsula, *Global and Planetary Change*, 71, 218-231,
 371 <https://doi.org/10.1016/j.gloplacha.2009.10.002>, 2010.
- 372 Naughton, F., Sanchez Goñi, M. F., Rodrigues, T., Salgueiro, E., Costas, S., Desprat,
 373 S., Duprat, J., Michel, E., Rossignol, L., Zaragosi, S., Voelker, A. H. L., and Abrantes,
 374 F.: Climate variability across the last deglaciation in NW Iberia and its margin,
 375 *Quaternary International*, 414, 9-22, <https://doi.org/10.1016/j.quaint.2015.08.073>, 2016.
- 376 Panagiotopoulos, K., Böhm, A., Leng, M. J., Wagner, B., and Schäbitz, F.: Climate
 377 variability over the last 92 ka in SW Balkans from analysis of sediments from Lake
 378 Prespa, *Climate of the Past*, 10, 643-660, <https://doi.org/10.5194/cp-10-643-2014>, 2014.
- 379 Pini, R., Ravazzi, C., and Donegana, M.: Pollen stratigraphy, vegetation and climate
 380 history of the last 215ka in the Azzano Decimo core (plain of Friuli, north-eastern Italy),
 381 *Quaternary Science Reviews*, 28, 1268-1290,
 382 <https://doi.org/10.1016/j.quascirev.2008.12.017>, 2009.
- 383 Rasmussen, S. O., Bigler, M., Blockley, S. P., Blunier, T., Buchardt, S. L., Clausen,
 384 H. B., Cvijanovic, I., Dahl-Jensen, D., Johnsen, S. J., Fischer, H., Gkinis, V., Guillevic,
 385 M., Hoek, W. Z., Lowe, J. J., Pedro, J. B., Popp, T., Seierstad, I. K., Steffensen, J. P.,
 386 Svensson, A. M., Vallenga, P., Vinther, B. M., Walker, M. J. C., Wheatley, J. J., and
 387 Winstrup, M.: A stratigraphic framework for abrupt climatic changes during the Last
 388 Glacial period based on three synchronized Greenland ice-core records: refining and
 389 extending the INTIMATE event stratigraphy, *Quaternary Science Reviews*, 106, 14-28,
 390 <https://doi.org/10.1016/j.quascirev.2014.09.007>, 2014.
- 391 Repschläger, J., Weinelt, M., Kinkel, H., Andersen, N., Garbe-Schönberg, D., and
 392 Schwab, C.: Response of the subtropical North Atlantic surface hydrography on deglacial



- 393 and Holocene AMOC changes, *Paleoceanography*, 30, 456-476,
 394 <https://doi.org/10.1002/2014pa002637>, 2015.
- 395 Sánchez Goñi, M. F., Desprat, S., Fletcher, W. J., Morales-Molino, C., Naughton, F.,
 396 Oliveira, D., Urrego, D. H., and Zorzi, C.: Pollen from the deep-sea: a breakthrough in
 397 the mystery of the Ice Ages, *Frontiers in plant science*, 9, 38,
 398 <https://doi.org/10.3389/fpls.2018.00038>, 2018.
- 399 Schulz, M., and Mudelsee, M.: REDFIT: estimating red-noise spectra directly from
 400 unevenly spaced paleoclimatic time series, *Computers & Geosciences*, 28, 421-426,
 401 [https://doi.org/10.1016/S0098-3004\(01\)00044-9](https://doi.org/10.1016/S0098-3004(01)00044-9), 2002.
- 402 Schulz, M., and Paul, A.: Holocene climate variability on centennial-to-millennial
 403 time scales: 1. Climate records from the North-Atlantic realm, in: *Climate development
 404 and history of the North Atlantic realm*, edited by: Wefer, G., Berger, W. H., Behre, K.-
 405 E., and Jansen, E., Springer, 41-54, 2002.
- 406 Sierro, F. J., Hodell, D. A., Curtis, J. H., Flores, J. A., Reguera, I., Colmenero-
 407 Hidalgo, E., Bárcena, M. A., Grimalt, J. O., Cacho, I., Frigola, J., and Canals, M.: Impact
 408 of iceberg melting on Mediterranean thermohaline circulation during Heinrich events,
 409 *Paleoceanography*, 20, 1-13, <https://doi.org/10.1029/2004pa001051>, 2005.
- 410 Soon, W., Connolly, R., and Connolly, M.: Re-evaluating the role of solar variability
 411 on Northern Hemisphere temperature trends since the 19th century, *Earth-Science
 412 Reviews*, 150, 409-452, <https://doi.org/10.1016/j.earscirev.2015.08.010>, 2015.
- 413 Stager, J. C., Ryves, D. B., Chase, B. M., and Pausata, F. S.: Catastrophic drought in
 414 the Afro-Asian monsoon region during Heinrich event 1, *Science*, 331, 1299-1302,
 415 <https://doi.org/10.1126/science.1198322>, 2011.
- 416 Stríkis, N. M., Chiessi, C. M., Cruz, F. W., Vuille, M., Cheng, H., de Souza Barreto,
 417 E. A., Mollenhauer, G., Kasten, S., Karmann, I., Edwards, R. L., Bernal, J. P., and Sales,
 418 H. d. R.: Timing and structure of Mega-SACZ events during Heinrich Stadial 1,
 419 *Geophysical Research Letters*, 42, 5477-5484A, <https://doi.org/10.1002/2015GL064048>,
 420 2015.



421 Turney, C., Baillie, M., Clemens, S., Brown, D., Palmer, J., Pilcher, J., Reimer, P.,
422 and Leuschner, H. H.: Testing solar forcing of pervasive Holocene climate cycles, Journal
423 of Quaternary Science: Published for the Quaternary Research Association, 20, 511-518,
424 <https://doi.org/10.1002/jqs.927>, 2005.

425 van Geel, B., Raspopov, O. M., Renssen, H., van der Plicht, J., Dergachev, V. A.,
426 and Meijer, H. A. J.: The role of solar forcing upon climate change, Quaternary Science
427 Reviews, 18, 331-338, [https://doi.org/10.1016/S0277-3791\(98\)00088-2](https://doi.org/10.1016/S0277-3791(98)00088-2), 1999.

428 Zhang, W., Wu, J., Wang, Y., Wang, Y., Cheng, H., Kong, X., and Duan, F.: A
429 detailed East Asian monsoon history surrounding the ‘Mystery Interval’ derived from
430 three Chinese speleothem records, Quaternary Research, 82, 154-163,
431 <https://doi.org/10.1016/j.yqres.2014.01.010>, 2014.

432



FIGURES AND FIGURE CAPTIONS

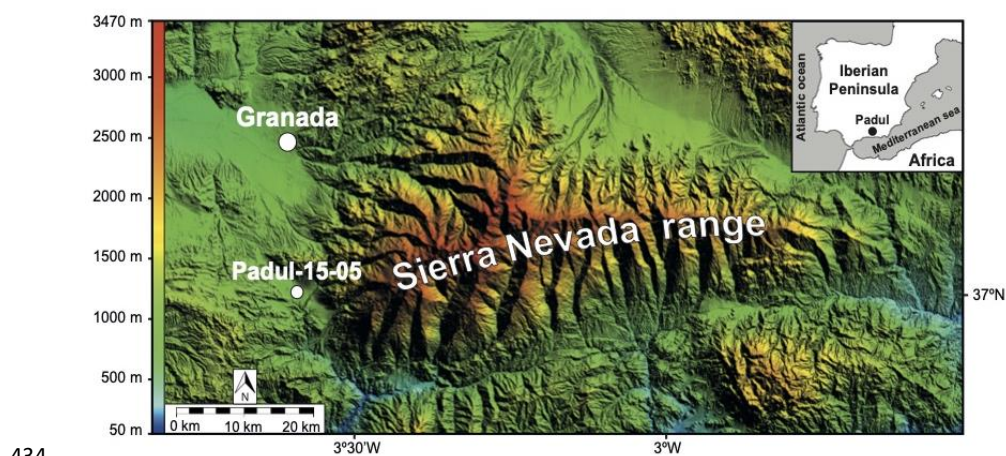
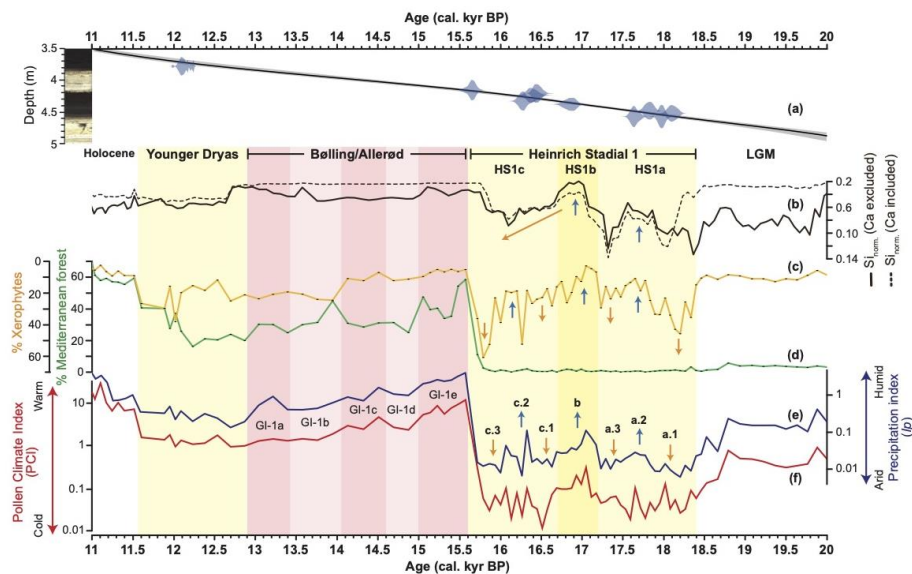
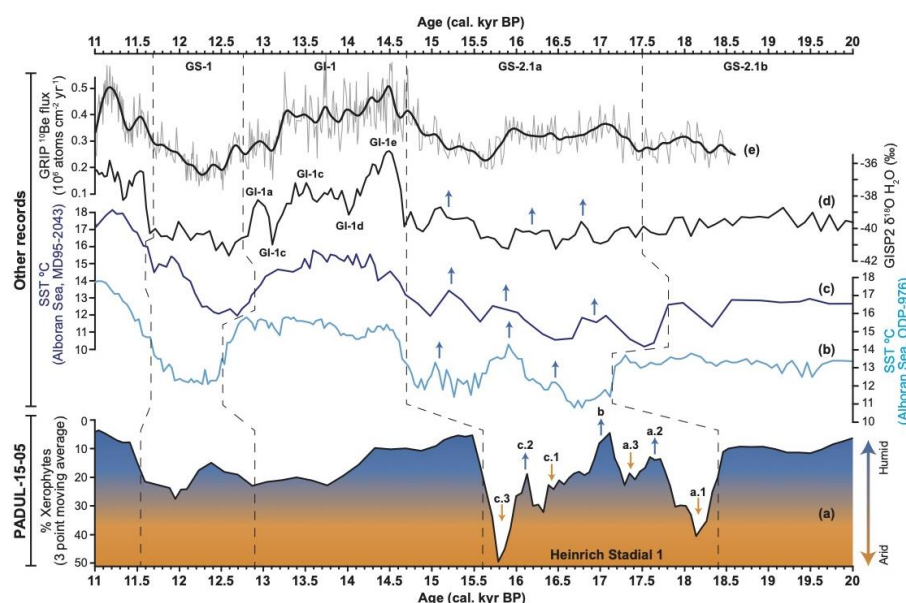


Figure 1. Geographical location of the Padul-15-05 record in the western margin of Sierra Nevada range and south of Granada city (southern Iberian Peninsula) (modified from Camuera et al., 2018).



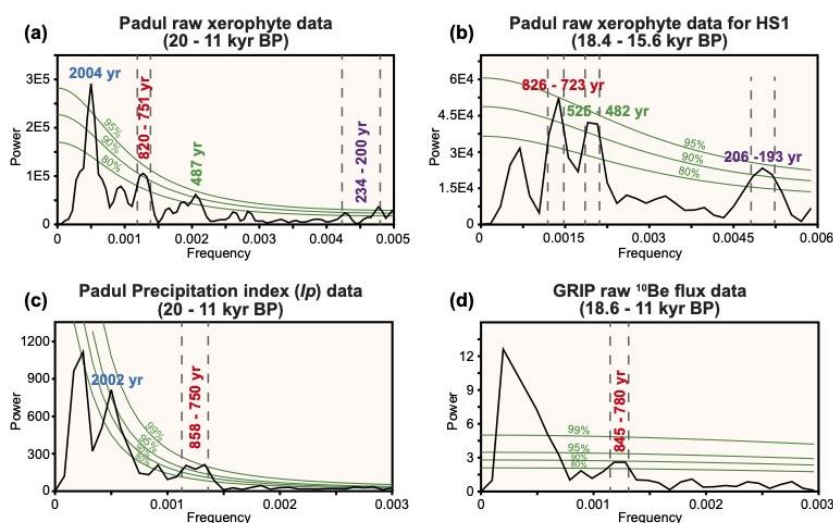
438

439 **Figure 2.** Paleoclimatic raw data from the Padul-15-05 sediment core for the time period
 440 between 20 and 11 kyr BP: (a) Photograph and age-depth model. (b) Normalized silicon
 441 values, with calcium excluded (continuous line) and included (dashed line) from total
 442 counts (values inverted) (Methods, Supplementary Information). (c) Percentage of
 443 xerophytes (values inverted). (d) Percentage of Mediterranean forest. (e) Precipitation
 444 Index (I_p). (f) Pollen Climate Index (PCI). Yellow shadings show the Younger Dryas
 445 (YD) and Heirich Stadial 1 (HS1). Dark yellow shading within HS1 indicates the slightly
 446 warmer/wetter middle phase (HS1b). Red and pink shadings show the Bølling-Allerød
 447 (BA). In particular, red shadings correspond to the warmer/wetter Greenland Interstadials
 448 1a, 1c and 1e, and pink shadings to the colder/more arid Greenland Interstadial 1b and
 449 1d. Blue arrows indicate moderately warmer/wetter sub-phases within HS1, whereas
 450 orange arrows show colder/more arid sub-phases.



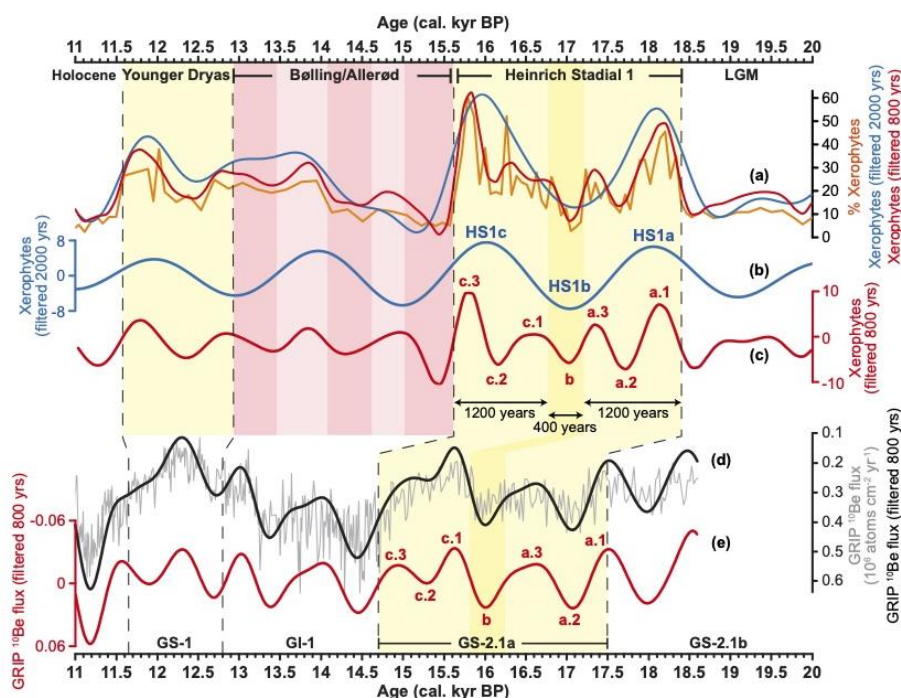
451

452 **Figure 3.** Paleoclimatic proxy data from Padul, Mediterranean Sea and Greenland ice-
 453 cores for the time period between 20 and 11 kyr BP: (a) Xerophyte data from Padul-15-
 454 05 with three-point moving average (values inverted). (b) SST (degrees Celsius) from
 455 ODP-976 record of Alboran Sea (Martrat et al., 2014). (c) SST (degrees Celsius) from
 456 MD95-2043 record of Alboran Sea (Cacho et al., 1999; 2006). (d) Raw $\delta^{18}\text{O}$ H_2O values
 457 (‰) from GISP2 (Grootes et al., 1993). (e) Raw ^{10}Be flux values (10^6 atoms cm^{-2} yr^{-1})
 458 (grey line) and smoothed data (black line) from GRIP (Adolphi et al., 2014). Within HS1,
 459 blue and orange arrows in the Padul record show the humid and arid phases, respectively.
 460 In the SSTs from Alboran Sea and the Greenland record during HS1, blue arrows marked
 461 the warmer temperatures in relation with the relatively more humid phases from Padul
 462 for this period (HS1a.2, HS1b and HS1c.2). Vertical dashed lines show transitions
 463 between LGM-HS1 (GS-2.1b – GS-2.1a), HS1-BA (GS-2.1a – GI-1), BA-YD (GI-1 –
 464 GS-1) and YD-Holocene for each study.



465

466 **Figure 4.** Cyclostratigraphic analysis of the Padul-15-05 pollen data and Greenland ice-
 467 core record during HS1. Spectral analysis run on: (a) Raw xerophyte percentages from
 468 the Padul-15-05 record for the age range between 20 and 11 kyr BP. (b) Raw xerophyte
 469 percentages for HS1 (18.4 – 15.6 kyr BP). (c) *Ip* data for the age period between 20 and
 470 11 kyr BP. (d) GRIP ^{10}Be flux data between 18.6 – 11 kyr BP. Note that the spectral peak
 471 of the GRIP ^{10}Be between 0.0001973 and 0.0005919 frequencies (a cycle with a
 472 periodicity between 5068 and 1689 years) seems to be an artefact, as the longer
 473 periodicity cycles (closer to 5 kyr) cannot be significant in a time series of data spanning
 474 7600 years.



475

476 **Figure 5.** (a) Raw percentages of xerophyte taxa (orange line) along with the filtered
 477 xerophyte taxa based on the obtained ~2000-yr cycle (blue line) and the ~800-yr cycle
 478 (red line) (see spectral analysis from Figure 4a and b). (b) Xerophyte data filtered using
 479 a bandwidth parameter of 0.0001 for the ~2000-yr cycle (blue line). (c) Xerophyte data
 480 filtered using a bandwidth parameter of 0.0006 for the ~800-yr cycle (red line). Note that
 481 the 3 main phases (HS1a, HS1b and HS1c) are marked within HS1 in relation with the
 482 ~2000-yr cycle, and the internal sub-phases (a.1-a.3, b, and c.1-c.3) in relation with the
 483 ~800-yr cycle. The length of the HS1a, HS1b and HS1c have also been marked. (d) GRIP
 484 ^{10}Be flux data (10^6 atoms $\text{cm}^{-2} \text{yr}^{-1}$; values inverted) (grey line) filtered to the obtained
 485 cyclicity of ~800 yr (black line) (see spectral analysis from Figure 4d). (G) GRIP ^{10}Be
 486 flux data filtered using a bandwidth parameter of 0.0006 for the ~800-yr cycle. Vertical
 487 dashed lines have been marked according to the Greenland Stadials (GS-2.1b, GS-2.1a,
 488 GS-1) and Interstadial (GI-1) delimitations (Rasmussen et al., 2014).